Schottky nanocontacts on ZnO nanorod arrays

W. I. Park and Gyu-Chul Yi[a)]
Department of Materials Science and Engineering, Pohang University of Science and Technology (POSTECH), Pohang, Kyoungbuk 790-784, Korea

J.-W. Kim and S.-M. Park
Department of Chemistry and Center for Integrated Molecular Systems, POSTECH, Pohang, Kyoungbuk 790-784, Korea

(Received 20 January 2003; accepted 22 April 2003)

We report on fabrication and electrical characteristics of ZnO nanorod Schottky diode arrays. High quality ZnO nanorods were grown for the fabrication of the Schottky diodes using noncatalytic metalorganic vapor phase epitaxy and Au was evaporated on the tips of the vertically well-aligned ZnO nanorods. $I-V$ characteristics of both bare ZnO and Au/ZnO heterostructure nanorod arrays were measured using current-sensing atomic force microscopy. Although both nanorods exhibited nonlinear and asymmetric $I-V$ characteristic curves, Au/ZnO heterostructure nanorods demonstrated much improved electrical characteristics: the reverse-bias breakdown voltage was improved from -3 to -8 V by capping a Au layer on the nanorod tips. The origin of the enhanced electrical characteristics for the heterostructure nanorods is suggested. © *2003 American Institute of Physics.* [DOI: 10.1063/1.1584089]

There has recently been great interest in the preparation and characterizations of one-dimensional (1D) semiconductor nanostructures for nanoscale electronic and optoelectronic device applications.[1,2] Both homogeneous, $p-n$ junction, and heteroepitaxial nanowires and nanorods have already been employed in several nanodevice prototypes.[3–6] Despite significant progress in the fabrication of nanodevices based on 1D nanomaterials, reliable nanoscale metal–semiconductor (M/SC) contacts are still required for miniaturization of device scales and increases in nanodevice density. In particular, a M/SC rectifying junction, called a Schottky barrier diode, is useful in electronic and optoelectronic device applications since Schottky barrier diodes generally exhibit shows faster switching and lower turn-on voltages than $p-n$ junction diodes.[7] Nevertheless, only little research has been performed on M/SC Schottky nanocontacts.[8–10] In this letter, we report on the fabrication and characterizations of ZnO Schottky nanodevice arrays.

Both ZnO and Au/ZnO nanorod arrays were prepared on $Al_2O_3(00\cdot1)$ substrates using a low-pressure metalorganic vapor phase epitaxy system and an electron-beam evaporation system. For ZnO nanorod growth, diethylzinc and oxygen were employed as the reactants.[11] No metal impurity catalyst was deposited on the substrates, excluding possible incorporation of metal impurities. Excellent crystallinity and optical properties of ZnO nanorods are reported elsewhere.[12,13] Prior to ZnO nanorod growth, in this research, 200–300-Å-thick ZnO buffer layers (with an electron concentration of 3×10^{18} cm^{-3}, a mobility of 30 $cm^2/V\,s$, and a resistivity of 0.07 $\Omega\,cm$) were initially deposited for easy formation of ohmic contacts for nanorod Schottky diode arrays. Ohmic contacts of the diode arrays were made annealing indium dots on the ZnO layers. Furthermore Au/ZnO heterostructure nanorod arrays were also fabricated by evaporating Au on the vertically aligned ZnO nanorod arrays.[14] The Au film deposition rate was in the range of 0.5–1 Å/s and typical Au film thicknesses were in the range of 100–300 Å, depending on film deposition time.

Topography and $I-V$ characteristic curve measurements of both bare and heterostructure nanorods were carried out using an atomic force microscope system.[15] For both measurements, a sharpened pyramidal Au-coated conducting tip with a spring constant of 0.12 N/m was employed. Atomic force microscopy (AFM) images were measured at a low contact force less than 10 nN in a contact mode, preventing possible damage of probe tips and samples, both the topography and electrical measurements were performed using the same tip. For $I-V$ measurements, current was measured at various bias voltages applied between the conducting tip and contact layers using current sensing module. All measurements were performed at room temperature under flowing nitrogen purge gas in a chamber. Each $I-V$ characteristic curve was plotted by measuring 20 times and averaging the data.

Electron microscopy images have revealed the general morphology of vertically well-aligned Au/ZnO heterostructure nanorod arrays [Figs. 1(a) and 1(b)]. Mean diameters and lengths of the nanorods were in the range of 30–40 nm and 1 μm, respectively. The general morphology in the scanning electron microscopy (SEM) images was not significantly changed by the metal deposition since metal atoms were adsorbed mainly on the top surfaces of nanorods exposed to the metal flux. The formation of Au layers on ZnO nanorods was clearly observed using transmission electron microscopy (TEM). As shown in Fig. 1(c), Au layers with typical thicknesses of 100–150 Å were formed mainly on top surfaces of ZnO nanorods while nanorod stems were rarely coated with Au. Prior to electrical characteristic measurements, the topography of ZnO nanorod arrays was obtained

a)Author to whom correspondence should be addressed; electronic mail: gcyi@postech.ac.kr

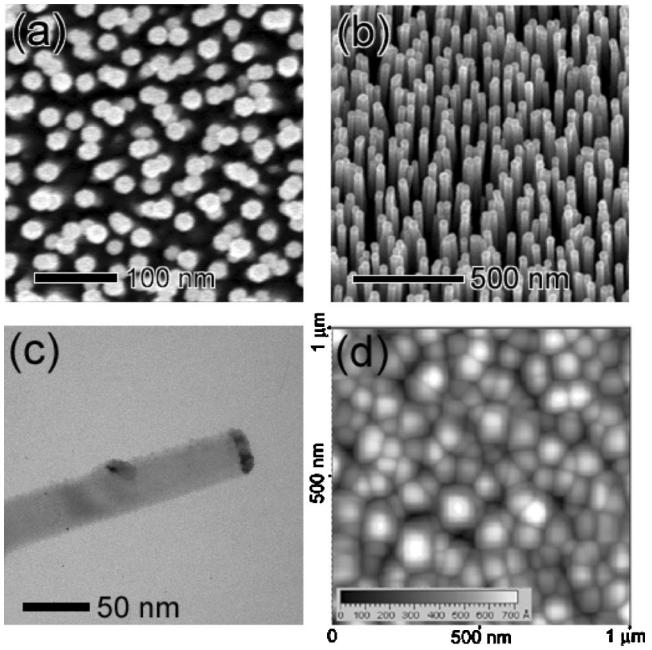

FIG. 1. (a) Plan-view, (b) tilted-view field-emission–SEM, (c) TEM, and (d) AFM images of Au/ZnO heterostructure nanorod arrays. The heterostructure nanorods show a mean diameters and lengths of 30–40 nm and 1 μm, respectively. From the TEM image, a Au layer with a thickness of 100 Å is shown only on ZnO nanorod tips. The Topography of Au/ZnO nanorod arrays was also obtained using an AFM contact mode.

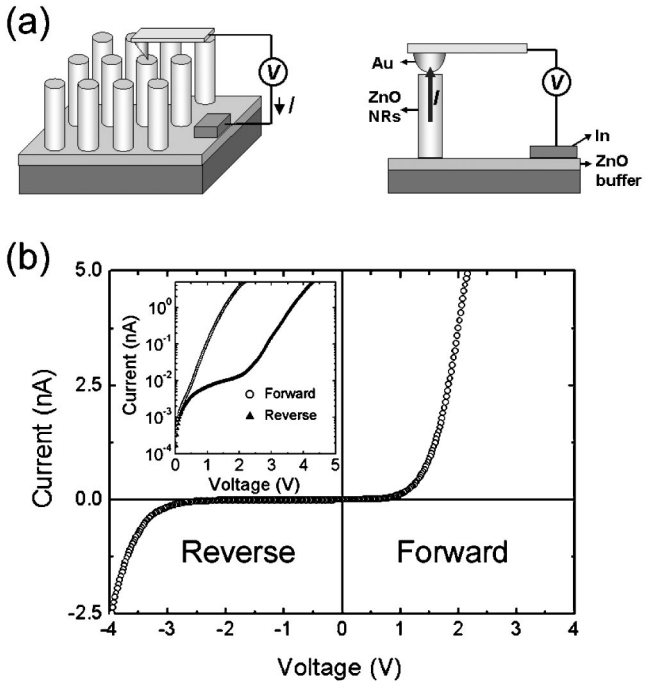

FIG. 2. (a) Schematic of current sensing AFM measurement and (b) typical $I-V$ characteristic curve of a bare ZnO nanorod. The inset shows a log I vs V plot. The $I-V$ characteristic curve is shown to be nonlinear and asymmetric.

using an AFM contact mode. As shown in Fig. 1(d), the AFM image of a ZnO nanorod array exhibits larger diameters of ZnO nanorods than those observed in SEM images. This distortion results from the tip convolution effect due to the high aspect ratio of the nanorods.[16] Electrical characteristics were measured on the hillocks in AFM images, which correspond to the tops of nanorod surfaces.

$I-V$ characteristic curves of bare ZnO nanorods were measured using current-sensing AFM (CSAFM). For these measurements, a M/SC point contact junction was formed by placing a Au-coated conducting tip on an individual ZnO nanorod top surface as shown in Fig. 2(a). The point contact on bare ZnO nanorods results in nonlinear and asymmetric behavior in their $I-V$ curves although the detailed shape of the curves depended on surface conditions as well as measurement parameters, e.g., the contact force of the tip. Figure 2(b) shows a typical $I-V$ characteristic curve measured on bare ZnO nanorods at a contact force of 21 nN. As shown in Fig. 2(b), the $I-V$ characteristic curve shows a turn-on voltage of 0.5–1 V for the forward bias and a reverse bias breakdown voltage of -3 V. The nonlinear and rectifying behavior in $I-V$ characteristics results from the Schottky contact formation of the Au-coated tip on a ZnO nanorod since Au on the AFM tip has a high work function of 5.1 eV and the built-in potential barriers in n-ZnO nanorod/n^+-ZnO buffer/indium (In) junction are quite negligible. However, a better M/SC junction must be prepared for the Schottky nanodiode applications since the point contact on bare ZnO nanorods exhibited poor reliability on electrical measurements and leads to easy breakdown at a low reverse voltage of -3 V.

The electrical characteristics of ZnO Schottky diodes were improved by deposition of a thin Au layer on ZnO nanorod tips. Figure 3(b) shows a typical $I-V$ characteristic curve measured on Au/ZnO heterostructure nanorod arrays, exhibiting clear rectifying behavior without significant reverse-bias breakdown up to -8 V. This significantly enhanced $I-V$ characteristic curve was routinely obtained at a contact force of 20–40 nN during repeated measurements on different nanorods. Since there is no contact potential barrier

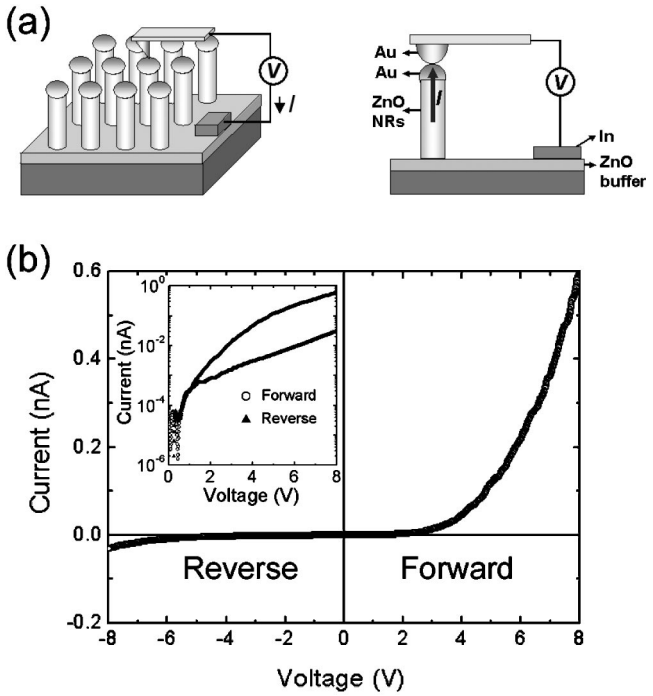

FIG. 3. (a) Schematic of current sensing AFM measurement and (b) typical $I-V$ characteristic curve of a Au/ZnO heterostructure nanorod. Inset shows log I vs V plot. The $I-V$ characteristic curve shows clear rectifying behavior without high current flow until the reverse-bias voltage increases up to -8 V.

between the Au tip and Au metal layer, the rectifying behavior in $I-V$ characteristics results from the Schottky contact formation between the Au and ZnO layers. Hence, the enhanced reliability and stability in the $I-V$ characteristic of the heterostructure nanorods results from the formation of a large area M/SC junction with a well-defined interface by Au layer deposition. From high-resolution TEM measurements, the interface between Au and ZnO layers has already been observed to be clean and abrupt.[14]

A typical $I-V$ characteristic of a Schottky barrier diode, neglecting series and shunt resistance, is describe by

$$I = I_s \exp\left(\frac{qV}{\eta K_B T} - 1\right), \tag{1}$$

where I_s is the reverse bias saturation current density, k_B is the Boltzmann's constant, T is the absolute temperature, and η is the ideality factor, close to unity for dominant thermionic emission of conventional Schottky diodes. For Au point contacts on bare ZnO nanorods, however, η was estimated to be 7–9 from the slope of ln(I) vs V plot [typically for $0.2 < V_f < 1$ V in inset of Figs. 2(b) and 3(b)]. The large deviation of ideality factor from unity strongly suggests that $I-V$ characteristics of both nanorod Schottky diodes are different from conventional Schottky diode behavior. Similar behavior has previously been reported for scanning tunneling microscope contact on bare Si semiconductor surfaces and $CoSi_2$ island/Si (111).[8–10]

As shown in Figs. 2(b) and 3(b), for the $I-V$ characteristic curves measured on bare ZnO nanorods, both reverse-bias breakdown voltage and diode resistance were much lower than those for Au/ZnO heterostructure nanorod Schottky diodes. This behavior presumably results from the small Au contact area formed by the sharp AFM probe tip for point contact junctions. In this case, a high electric field is generally induced directly on the ZnO top surface beneath the contact point due to the sharp curvature of Au-coated probe tips and, hence, the Schottky barrier thickness decreases, resulting in easy electron tunneling across M/SC interface. For such small diodes of the point contact junction, the Schottky barrier thickness decreases with decreasing diode size as previously suggested by Smit *et al.*[10] In contrast, the junction area for Au/ZnO heterostructure Schottky diodes becomes much larger and so the electric field is uniformly spread on the Au metal layer, which results in a decreased tunneling current between Au and ZnO and an increase in the reverse-bias breakdown voltage.

In summary, ZnO nanorod Schottky diode arrays were fabricated and their current–voltage characteristics were measured by placing a Au-coated conducting tip on individual nanorod top surfaces using CSAFM. Although both bare ZnO and Au/ZnO heterostructure nanorods exhibited nonlinear and asymmetric $I-V$ characteristic curves, Au/ZnO heterostructure nanorods demonstrated much improved electrical characteristics: the reverse-bias breakdown voltage was improved from -3 to -8 V by capping a Au layer on the nanorod tips, presumably due to an increase in the junction area and the formation of well-defined interface between Au and ZnO layers.

This work was supported by the Nano R&D national project (Contract No. M10214000115-02B1500-01910).

[1] S. W. Chung, J. Y. Yu, and J. R. Heath, J. Phys. Chem. B **104**, 11864 (2000).
[2] Y. Cui and C. M. Lieber, Science **291**, 851 (2001); J. F. Wang, M. S. Gudiksen, X. F. Duan, Y. Cui, and C. M. Lieber, *ibid.* **293**, 1455 (2001); Y. Cui, Q. Q. Wei, H. K. Park, and C. M. Lieber, *ibid.* **293**, 1289 (2001); X. Duan, Y. Huang, Y. Cui, J. Wang, and C. M. Lieber, Nature (London) **409**, 66 (2001).
[3] J. Hu, M. Ouyang, P. Yang, and C. M. Lieber, Nature (London) **399**, 48 (1999); M. S. Gudiksen, L. J. Lauhon, J. Wang, D. C. Smith, and C. M. Lieber, *ibid.* **415**, 617 (2002).
[4] Y. Wu, R. Fan, and P. Yang, Nano Lett. **2**, 83 (2002).
[5] M. T. Bjork, B. J. Ohlosson, T. Sass, A. I. Persson, C. Thelander, M. H. Magnusson, K. Deppert, L. R. Wallenberg, and L. Samuelson, Nano Lett. **2**, 87 (2002).
[6] W. I. Park, G.-C. Yi, M. Kim, and S. J. Pennycook, Adv. Mater. (Weinheim, Ger.) **15**, 526 (2003).
[7] S. Sze, *Physics of Semiconductor Devices*, 2nd ed. (Wiley, New York, 1981).
[8] P. Avouris, I.-W. Lyo, and Y. Hasegawa, J. Vac. Sci. Technol. A **11**, 1725 (1993).
[9] R. Hasunuma, T. Komeda, and H. Tokumoto, Appl. Surf. Sci. **84**, 130 (1998).
[10] G. D. J. Smit, S. Rogge, and T. M. Klapwijk, Appl. Phys. Lett. **80**, 2568 (2002); **81**, 3852 (2002).
[11] W. I. Park, D. H. Kim, S. W. Jung, and G.-C. Yi, Appl. Phys. Lett. **80**, 4232 (2002).
[12] W. I. Park, G.-C. Yi, M. Kim, and S. J. Pennycook, Adv. Mater. (Weinheim, Ger.) **14**, 1841 (2002).
[13] W. I. Park, Y. H. Jun, S. W. Jung, and G.-C. Yi, Appl. Phys. Lett. **82**, 964 (2003).
[14] W. I. Park, S. W. Jung, G.-C. Yi, S. H. Oh, C. G. Park, and M. Kim, Jpn. J. Appl. Phys., Part 2 **41**, L1206 (2002).
[15] D. J. Wold and C. D. Frisbie, J. Am. Chem. Soc. **123**, 5549 (2001). J. Li, R. Stevens, L. Delzeit, H. T. Ng, A. Cassell, J. Han, and M. Meyyappan, Appl. Phys. Lett. **81**, 910 (2002).
[16] J. S. Villarrubia, J. Res. Natl. Inst. Stand. Technol. **102**, 425 (1997).